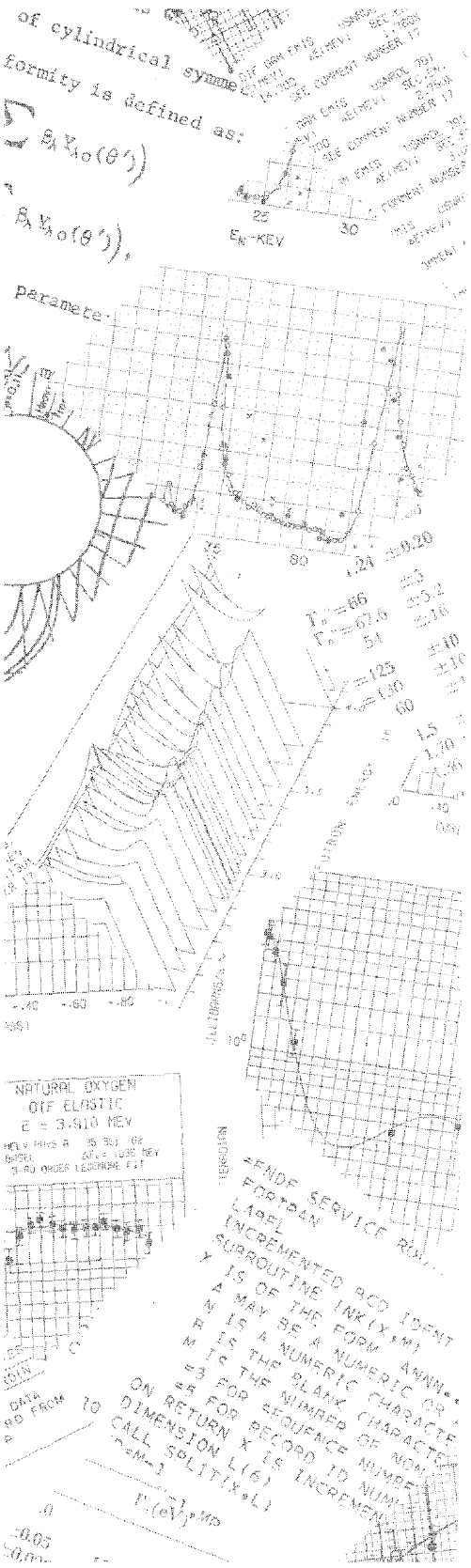

BNL 50442
(ENDF-208)

EVALUATION OF THE NEUTRON AND GAMMA-RAY PRODUCTION CROSS-SECTIONS FOR ^{55}Mn

HIROSHI TAKAHASHI

November 1974

NATIONAL NEUTRON CROSS SECTION CENTER
BROOKHAVEN NATIONAL LABORATORY
UPTON, NEW YORK 11973

National
Neutron
Cross
Section
Center

BNL 50442
(ENDF-208)
(Physics-Nuclear - TID-4500)

EVALUATION OF THE NEUTRON AND GAMMA-RAY CROSS-SECTIONS FOR ^{55}Mn

HIROSHI TAKAHASHI

November 1974

NATIONAL NEUTRON CROSS SECTION CENTER
BROOKHAVEN NATIONAL LABORATORY
ASSOCIATED UNIVERSITIES, INC.
UNDER CONTRACT NO. AT(30-1)-16 WITH THE
U.S. ENERGY RESEARCH AND DEVELOPMENT ADMINISTRATION

NOTICE

Printed in the United States of America
Available from
National Technical Information Service
U.S. Department of Commerce
5285 Port Royal Road
Springfield, VA 22161
Price: Printed Copy, Domestic $10.00;
Foreign $12.50; Microfiche $1.45

March 1975 365 copies

Contents

List of Tables

List of Illustrations

1. Introduction

This report summarizes the evaluation of neutron and gamma-ray production cross sections for Mn^{55} from 1.0 x 10^{-5}eV to 20.0 MeV for ENDF/B-IV.

The resolved resonance parameters and the associated smooth background in File 3 are taken over from the ENDF/B-II (MAT=1019) evaluation. In addition, the neutron cross-sections at higher energies have been reevaluated and the gamma-ray production cross-sections have been added.

2. General Information (File 1)

2.1 General Identification

Mn 55

MAT = 1197

ZA = 25055.0

AWR = 149.623

R = 0.454 x 10^{-12}cm

I = 2.5

and the (n, particle) Q values are given in Table 1.

2.2 Radioactive Decay (MT = 453)

The data of radioactive decay have remained the same as the data of ENDF/B-II. The data were not newly evaluated.

3. Resonance Parameters (File 2)

3.1 Resolved Resonance Region

Since an extensive study of the available experimental and the calculated cross-section was carried out in evaluating the resolved resonance region of the ENDF/B-II evaluation (MAT=1019), it was decided to retain these resonance parameters and the associated background in File 3. The only change made in these parameters was to reduce the gamma-width from 0.52 eV to 0.516 eV.

The thermal capture cross-section calculated from these parameters is 13.3 barns and the capture resonance integral from 0.5 eV up is 15.31 barns.

3.2 Unresolved Resonance Region

No unresolved resonance parameters are given in this evaluation.

4. Neutron Cross Sections (File 3)

4.1 Total Cross Section (MT = 1)

From 1.0-05 eV to 80 keV, the cross section is given by the resolved resonance parameters. Above this energy, the cross section up to 500.0 keV was based on the Stubbin's data[3] and Rohr et al's data[2]. The cross section from 500 keV to 20.0 MeV was based on the KFK Cierjack's data[4]. The cross-sections were obtained by spline fit to the experimental data.

4.2 Elastic Scattering Cross Section (MT = 2)

The elastic scattering cross sections in the energy range higher than the resolved resonance energy were obtained by subtracting the non-elastic cross section from the evaluated total cross section.

4.3 Nonelastic Scattering Cross Section (MT = 3)

The nonelastic scattering cross section was calculated by summing up all cross sections except the elastic scattering cross section.

4.4 Inelastic Scattering Cross Section (MT = 4, 51, 52 ..., 91)

The inelastic scattering cross sections were given as total (MT = 4), discrete level excitation cross sections (MT = 51 ...) of the first 5 levels and continuum level excitation cross section (MT = 91). The level scheme for these discrete levels was taken from the data of ref (5), and is tabulated in Table 2.

The individual excitation functions calculated by using the COMNUC-3 codes[6] give good agreement with the experimental data[7]-[12], so that these

calculated values are taken as the evaluated values. The optical model parameters used in this calculation will be described in the section on the optical model. The cross sections of the individual discrete levels are given up to 9 MeV. Above this energy the cross sections are set equal to zero by neglecting the direct process. An improvement for the evaluation can be done using the coupled-channel calculation by Jupitor code[13]. For the inelastic scattering cross section which excites the continuum of levels, the evaluated data are taken from the calculated results of COMNUC-3 and GRØGI-III[14].

4.5 (n,p) and (n,n'p) Cross Sections (MT=103, 28)

Most of the experiments for the (n,p) cross section were carried out around 14 MeV (Ref. 16-21). The cross sections calculated by using the COMNUC-3 and GRØGI-III codes were taken as the evaluated data. The cross section of (n,n'p) reaction was calculated by GRØGI-III code.

4.6 (n,α) and (n,n'α) Cross Section (MT=1071,22)

The (n,α) cross sections in the neutron energy range between 12 MeV and 19 MeV have been measured by F. Gabbard et al[22] and M. Bormann et al[23]. The cross sections of Gabbard et al are larger than Bormann's data in the low energy region from 12 to 14 MeV, but the former become smaller than the latter in the high energy range. The cross sections of Gabbard show strong structure. The other data[24]-[27] are scattered above or below these two data sets but the recent data show rather smaller values.

The nuclear model calculations using the statistical model codes GRØGI-III, COMNUC-3 and the semi empirical statistical model code THRESH[28] were performed. The calculations using GRØGI-3 code were carried out using two optical potential parameters of Becchetti and Greenlees[29] and Igo-Huizenga.

The cross section obtained from the latter potential shows the lower cross section. The cross sections calculated by THRESH code are larger than those calculated by Becchetti and Greenlees[29] parameters in the neutron energy range from 12 MeV to 20 MeV.

In the energy range less than 12 MeV, there are no experimental data, so that we evaluated the cross section in this range by model calculations. The statistical models used--GRØGI-III and THRESH are not accurate near the low energy region. So that the calculated value obtained from COMNUC-3 code is used as evaluated data.

4.7 (n,2n), (n,3n) Cross Sections (MT=16) (MT=17)

The (n,2n) activation cross section of Mn^{55} in the neutron range from 12.6 to 19.6 MeV has been measured by Menlove et al[30] and A. Paulsen, H. Liskien[31]. The other data for the cross sections were obtained either at one energy around the 14 MeV or measured over the fission neutron spectrum[32].

The Paulsen et al's data are about 15% higher than the Menlove's data and also show small fluctuations. The Paulsen's experiment was performed by using the proton recoil telescope technique to measure the absolute flux, and the Menlove's data are obtained from the ratio measurements to the U^{235} fission cross section.

These cross sections were evaluated by comparing these with the results calculated by using the nuclear model codes GRØGI-III and THRESH.

There are no experimental data near the threshold energy, and GRØGI-III code cannot treat the discrete excited level, so that the cross sections near the threshold were carefully evaluated by using the transmission coefficients obtained from optical model calculations. The (n,3n) cross section calculated from the GRØGI-III code was taken as evaluated cross section.

4.8 (n,d) Reaction Cross Section (MT=104)

(n,d) reaction cross section curve is calculated by the THRESH code and it is normalized to the experimental value of reference (33).

4.9 (n,He^3) Reaction Cross Section (MT=106)

(n,He^3) reaction cross sections are evaluated by referring to the experimental values of Refs (34, 35, & 36).

4.10 The Radiative Capture Cross Section (MT=102)

The radiative capture cross section up to 80 keV neutron energy is given by the resonance parameters as discussed above. The neutron capture cross section above 0.5 MeV was calculated by using the statistical model code COMNUC-3 with Axel's γ-ray strength function which deviates from the experimental value in the same way as shown by Devbenko's calculation[37]. So that the cross sections between 0.1 MeV and 2.5 MeV was evaluated mostly from the experimental data[37]-[41] but the small structure due to the opening of the inelastic neutron channels were taken into account by the results of the COMNUC-3 calculations. The cross sections between 2.5 MeV and 10 MeV were evaluated from the Menlove et al data and the ones from 10 MeV to 20 MeV were based on the Longo-Saporetti's[42] semi-direct process calculations. The capture cross-section is shown in Fig. 1.

5. Angular Distribution of Secondary Neutrons (File 4)

5.1 Elastic Scattering (MT = 2)

For neutron energy up to 8.05 MeV, the angular distributions measured by S. Cox[43] and B. Holmqvist[44] et al were taken as the evaluated data. These are shown in the BNL-400[45]. Above this energy up to 20 MeV, the shape elastic scattering calculated by the optical model code ABACUS-2[46] using the Becchetti-Greenlees's optical parameters was adopted as the evaluated data.

The Legendre coefficients calculated by CHAD were given in File 4.

5.2 Inelastically Scattered Neutrons (n,2n), (n,3n), (n,n'p) and (n,n'α) reactions (MT=51,...,91,MT=16,17,22,23)

Neutrons from these reactions were assumed to be isotropic in the center of mass system.

6. Energy Distribution of Secondary Neutrons (File 5)

6.1 (n,2n), (n,3n) and (n,n') reactions (MT=16,17, and 91)

The energy distribution of neutrons from the (n,2n), (n,3n) and the inelastic scattering cross section of the continuum part were assumed to have the form of an evaporation spectrum. The effective temperature of these evaporation spectra were obtained by GRØGI-III codes.

7. Multiplicities and Transition Probability Array of Gamma-Rays (File 12)

7.1 Radiative Capture Gamma-Ray Multiplicity

The gamma-ray spectra due to thermal neutron capture in ^{55}Mn isotope were measured by Hughes, et al.[47], Groshev et al[48]; Bartholomew et al[49] and Rasmussen et al[50] [51] [52] [53]. The evaluated data were taken mostly from Groshev's data. For the epithermal resonance capture, the high energy γ-ray spectra measured by R. Chrien et al[53] and P. Van Assche et al[54] were used as the evaluated data. The multiplicities increase as a function of incident neutron energy to preserve the total energy release. There are no experimental data for neutron energies larger than 1 MeV. So the gamma-ray production cross sections for all reactions were calculated by the GRØGI-III code. The multiplicities are tabulated in this file.

7.2 Transition Probability Array for Gamma-Ray due to Inelastic Neutron Scattering

The electro-magnetic transition probabilities from the excited levels of ^{55}Mn isotope were measured by several authors[56]-[58]. The evaluated

transition probabilities were calculated from these data.

8. Angular Distribution of Gamma-Ray (File 14)

All gamma-rays produced by neutron capture (MT=102), inelastic neutron scattering (MT=51∿55) and non elastic scattering (MT=3) are assumed to be isotropic.

9. Energy Distribution of Secondary Gamma-Rays (File 15)

The energy distribution of the secondary gamma-rays due to thermal neutron capture were expressed by a histogram type of spectrum with 0.25 MeV bin energy width. The ones due to the non elastic scattering for the neutron energy more than 1 MeV are tabulated as histogram type of spectrum with 0.5 MeV bin energy width.

10. Nuclear Model Calculations

10.1 Optical Model Parameter

In this evaluation work, optical model calculation has been used to obtain the neutron, proton and α particles penetrabilities. A spherical optical potential in the following form was used.

$$U(r) = V_c - Vf(x) + \left(\frac{h}{M_\pi C}\right)^2 V_{so}(\sigma \cdot \ell)\frac{1}{r}\frac{d}{dr} f(x_{so}) - i\left[WF(x_w) - 4W_D \frac{d}{dx_D} f(x_D)\right]$$

where

$$V_c = ZZ'e^2/r \qquad r \geq R_c$$

$$= (ZZ'e^2/2R_c)(3 - r^2/R_c^2) \qquad r \leq R_c$$

$$R_c = r_c A^{1/3}$$

$$f(x) = (1 + e^{x})^{-1} \text{ where } x = (r - r_o A^{1/3})/a$$

$$\left(\frac{h}{M_\pi C}\right)^2 = 2.0 \text{ (fermi)}^2$$

The neutron parameters at a neutron energy E_n(MeV) are mostly taken from Becchetti and Greenlees[6] data, which is shown as follows:

$V = 56.3 - 0.32E - 24(N-Z)/A$

$r_o = 1.17 \quad a = 0.75$

$W = 0.22E - 1.56$ or zero whichever is greater

$W_D = 13 - 0.25E - 12(N - Z)/A$, or zero whichever is greater

$r_W = r_D = 1.26 \quad a_W = a_D = 0.58$

$V_{so} = 6.2$

$r_{so} = 1.1 \quad a_{so} = 0.75$

where the unit of length is in Fermis.

For protons, the following parameters are used:

$V = 54. - 0.32 + 24(N-Z)/A + 0.4(Z)/A^{1/3}$

$r_o = 1.17 \quad a = 0.75$

$W = 0.22E - 2.7$, or zero, whichever is greater.

$W_D = 11.8 - 0.25E + 12(N-Z)/A$, or zero, whichever is greater.

$r_W = r_D = 1.32, \quad a_W = a_D = 0.51 + 0.7(N-Z)/A$

$V_{so} = 6.2$

$r_{so} = 1.01, \quad a_{so} = 0.75$

The alpha parameters are taken from the data obtained by C. R. Bingham et al.[59]

$V = 200 \quad W = 102.9$

$r_o = 1.254 \quad r_W = 1.254$

$$f(x) = (1 + e^{x})^{-1} \text{ where } x = (r - r_o A^{1/3})/a$$

$$\left(\frac{h}{M_\pi C}\right)^2 = 2.0 \text{ (fermi)}^2$$

The neutron parameters at a neutron energy E_n(MeV) are mostly taken from Becchetti and Greenlees[6] data, which is shown as follows:

$V = 56.3 - 0.32E - 24(N-Z)/A$

$r_o = 1.17 \quad a = 0.75$

$W = 0.22E - 1.56$ or zero whichever is greater

$W_D = 13 - 0.25E - 12(N - Z)/A$, or zero whichever is greater

$r_W = r_D = 1.26 \quad a_W = a_D = 0.58$

$V_{so} = 6.2$

$r_{so} = 1.1 \quad a_{so} = 0.75$

where the unit of length is in Fermis.

For protons, the following parameters are used:

$V = 54. - 0.32 + 24(N-Z)/A + 0.4(Z)/A^{1/3}$

$r_o = 1.17 \quad a = 0.75$

$W = 0.22E - 2.7$, or zero, whichever is greater.

$W_D = 11.8 - 0.25E + 12(N-Z)/A$, or zero, whichever is greater.

$r_W = r_D = 1.32, \quad a_W = a_D = 0.51 + 0.7(N-Z)/A$

$V_{so} = 6.2$

$r_{so} = 1.01, \quad a_{so} = 0.75$

The alpha parameters are taken from the data obtained by C. R. Bingham et al.[59]

$V = 200 \quad W = 102.9$

$r_o = 1.254 \quad r_W = 1.254$

12. Evaluated Cross-Sections

In addition to the evaluated capture cross-section of ^{55}Mn shown in Fig. 2 - 4 show plots of the remaining evaluated cross-sections from the data files.

The Legendre coefficients calculated by CHAD were given in File 4.

5.2 Inelastically Scattered Neutrons (n,2n), (n,3n), (n,n'p) and (n,n'α) reactions (MT=51,...,91,MT=16,17,22,23)

Neutrons from these reactions were assumed to be isotropic in the center of mass system.

6. Energy Distribution of Secondary Neutrons (File 5)

6.1 (n,2n), (n,3n) and (n,n') reactions (MT=16,17, and 91)

The energy distribution of neutrons from the (n,2n), (n,3n) and the inelastic scattering cross section of the continuum part were assumed to have the form of an evaporation spectrum. The effective temperature of these evaporation spectra were obtained by GRØGI-III codes.

7. Multiplicities and Transition Probability Array of Gamma-Rays (File 12)

7.1 Radiative Capture Gamma-Ray Multiplicity

The gamma-ray spectra due to thermal neutron capture in ^{55}Mn isotope were measured by Hughes, et al.[47], Groshev et al[48]; Bartholomew et al[49] and Rasmussen et al[50] [51] [52] [53]. The evaluated data were taken mostly from Groshev's data. For the epithermal resonance capture, the high energy γ-ray spectra measured by R. Chrien et al[53] and P. Van Assche et al[54] were used as the evaluated data. The multiplicities increase as a function of incident neutron energy to preserve the total energy release. There are no experimental data for neutron energies larger than 1 MeV. So the gamma-ray production cross sections for all reactions were calculated by the GRØGI-III code. The multiplicities are tabulated in this file.

7.2 Transition Probability Array for Gamma-Ray due to Inelastic Neutron Scattering

The electro-magnetic transition probabilities from the excited levels of ^{55}Mn isotope were measured by several authors[56]-[58]. The evaluated

22. F. Gabbard and B. D. Kern. Phys. Rev. 128, 1276 (1962).

23. M. Bormann. Nucl. Phys. 63, 438 (1963).

24. I. Kumabe. J. Phys. Soc. Japan 13, 325 (1958).

25. A. Peil. Nucl. Phys. 66, 419 (1965).

26. B. Minetti et. al. Zeit f. Physik 199, 275 (1967).

27. E. Frevert. Aeta. Phys. Austriaca, 20, 304 (1965).

28. S. Pearlstein. J. Nucl. Energy 27, 81 (1973).

29. F. D. Becchetti and G. W. Greenlees. Phys. Rev. 182, 1190 (1969).

30. H. Menlove et. al. Phys. Rev. 163, 1308 (1967).

31. A. Paulsen and H. Liskien. J. Nucl. Energy A/B19, 907 (1965).

32. M. Bormann et. al. Nucl. Phys. A130, 195 (1969).

33. L. Colli et. al. Nucl. Phys. 46, 73 (1963).

34. E. Bramlitt et. al. Phys. Rev. 125, 297 (1962).

35. I. Kumabe et. al. Phys. Rev. 117, 1568 (1960).

36. E. Frevert, Private Communication (1963).

37. A. Dovbenko et. al. J. Atomic Energy 26, 67 (1969).

38. Yu. Stavisskii, V. Tolstikov. J. Atomic Energy, 10, 508 (1961).

39. A. Johnsrud et. al. Phys. Rev. 116, 927 (1959).

40. D. Stupegia et. al. J. Nucl. Energy 22, 267 (1968).

41. H. Menlove et. al. Phys. Rev. 163, 1299 (1967).

42. G. Longo and F. Saporetti. Nucl. Phys. A127, 503 (1969).

43. B. Holmqvist and T. Wiedling. AE-366 (1969).

44. S. Cox, Private Communication, CSISRS AN/52198 (1966).

45. D. Garber et. al. BNL-400, Third Edn. Vol. II (1970).

46. E. Auerbach, BNL-6562 (1962).

47. L. B. Hughes et. al. Nucl. Phys. 80, 131 (1966).

48. L. Groshev *et. al.* Atlas of Thermal Neutron Capture Gamma Rays, Atomizdat, Moscow (1958).

49. G. Gartholomew and L. Higgs. AECL-668 (1958).

50. N. Rasmussen et. al. GA-10248 (DASA-2570) (1970).

51. G. Bartholomew et. al. Nuclear Data A3, 367 (1967).

52. O. A. Wasson et. al. Phys. Rev. 136, B1640 (1964).

53. R. Greenwood. IN-1407.

54. R. E. Chrien *et. al.* BNL-14246 (1969).

55. P. Van Assche et. al. Nucl. Phys. A160, 367 (1971).

56. N. Nath et. al. Nucl. Phys. 13, 74 (1959).

57. R. L. Auble *et. al.* Nucleas Data B3-3, 4-2 (1970).

58. J. Daniel et. al. Can. J. Phys. 46, 1849 (1968).

59. C. R. Bingham, M. Halbert and A. Quinton. Phys. Rev. 180, 1197 (1969).

Table 1. Q Values and Thresholds for Several Neutron Reactions on ^{55}Mn.

Reaction	Q (MeV)	Threshold (MeV)
$^{55}Mn(n,n)^{55}Mn$	0.	0.
$^{55}Mn(n,n')^{55}Mn^*$	- 0.12580	0.128117
$^{55}Mn(n,\gamma)^{56}Mn$	+ 7.2704	0.
$^{55}Mn(n,p)^{55}Cr$	- 1.8097	1.84281
$^{55}Mn(n,d)^{54}Cr$	- 5.8388	5.94735
$^{55}Mn(n,\ ^3He)^{53}V$	-12.3796	12.6067
$^{55}Mn(n,\alpha)^{52}V$	- 0.6216	0.63301
$^{55}Mn(n,n'\alpha)^{51}V$	- 7.9306	8.0762
$^{55}Mn(n,n'p)^{54}Cr$	- 8.0633	8.21260
$^{55}Mn(n,2n)^{54}Mn$	-10.225	10.4127
$^{55}Mn(n,3n)^{53}Mn$	-19.1680	19.5199

Table 2.

Nuclear Level Structure of ^{55}Mn

E_{ex} (MeV)	J^{π}
0.0	$5/2^-$
0.1258	$7/2^-$
0.984	$9/2^-$
1.292	$11/2^-$
1.528	$3/2^-$
1.883	$5/2^-$

Table 3
*Estimated Uncertainties in the Evaluated Cross Section of Mn-55**

Cross Section	ENDF/B Designation MF	MT	Neutron Energy (eV) Thermal	1	10^4	10^5	$3x10^5$	10^6	$3x10^6$	10^7	$1.4x10^7$	$2.0x10^7$
Total	3	1	6	10	5	5	5	5	5	3	3	3
Elastic	3	2	6	15	10	10	10	10	10	10	10	10
Non-elastic	3	3	3	5	10	10	10	10	10	10	10	10
Total (n,n')	3	4	-	-	-	-	10	10	10	10	-	-
Discrete (n,n')	3	51-55	-	-	-	-	15	15	15	-	-	-
Continuum (n,n')	3	91	-	-	-	-	-	-	10	10	-	-
(n,2n)	3	16	-	-	-	-	-	-	-	15	10	10
(n,3n)	3	17	-	-	-	-	-	-	-	-	-	40
(n,n'α)	3	22	-	-	-	-	-	-	-	400	400	400
(n,n'p)	3	28	-	-	-	-	-	-	-	400	400	400
(n,γ)	3	102	3	5	10	10	10	10	15	20	30	30
(n,p)	3	103	-	-	-	-	-	-	-	30	30	30
(n,d)	3	104	-	-	-	-	-	-	300	300	300	300
(n,He^3)	3	106	-	-	-	-	-	-	-	-	400	400
(n,α)	3	107	-	-	-	-	-	-	-	20	20	20
$Total_{(n,x\gamma)}$	12	3+102	10	20	20	20	20	30	30	30	30	30

* Percentage errors.

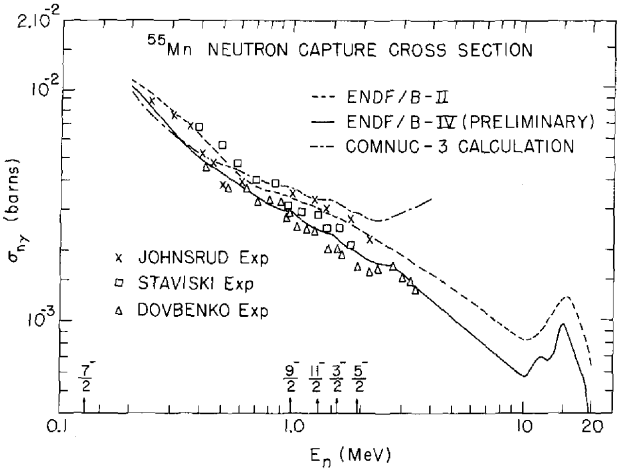
^{55}Mn NEUTRON CAPTURE CROSS SECTION
--- ENDF/B-II
— ENDF/B-IV (PRELIMINARY)
-·- COMNUC-3 CALCULATION
x JOHNSRUD Exp
□ STAVISKI Exp
△ DOVBENKO Exp
$\sigma_{n\gamma}$ (barns)
E_n (MeV)
2.10^{-2}
10^{-2}
10^{-3}
0.1
1.0
10
20
$\frac{7}{2}^-$
$\frac{9}{2}^-$
$\frac{11}{2}^-$
$\frac{3}{2}^-$
$\frac{5}{2}^-$

Figure 1

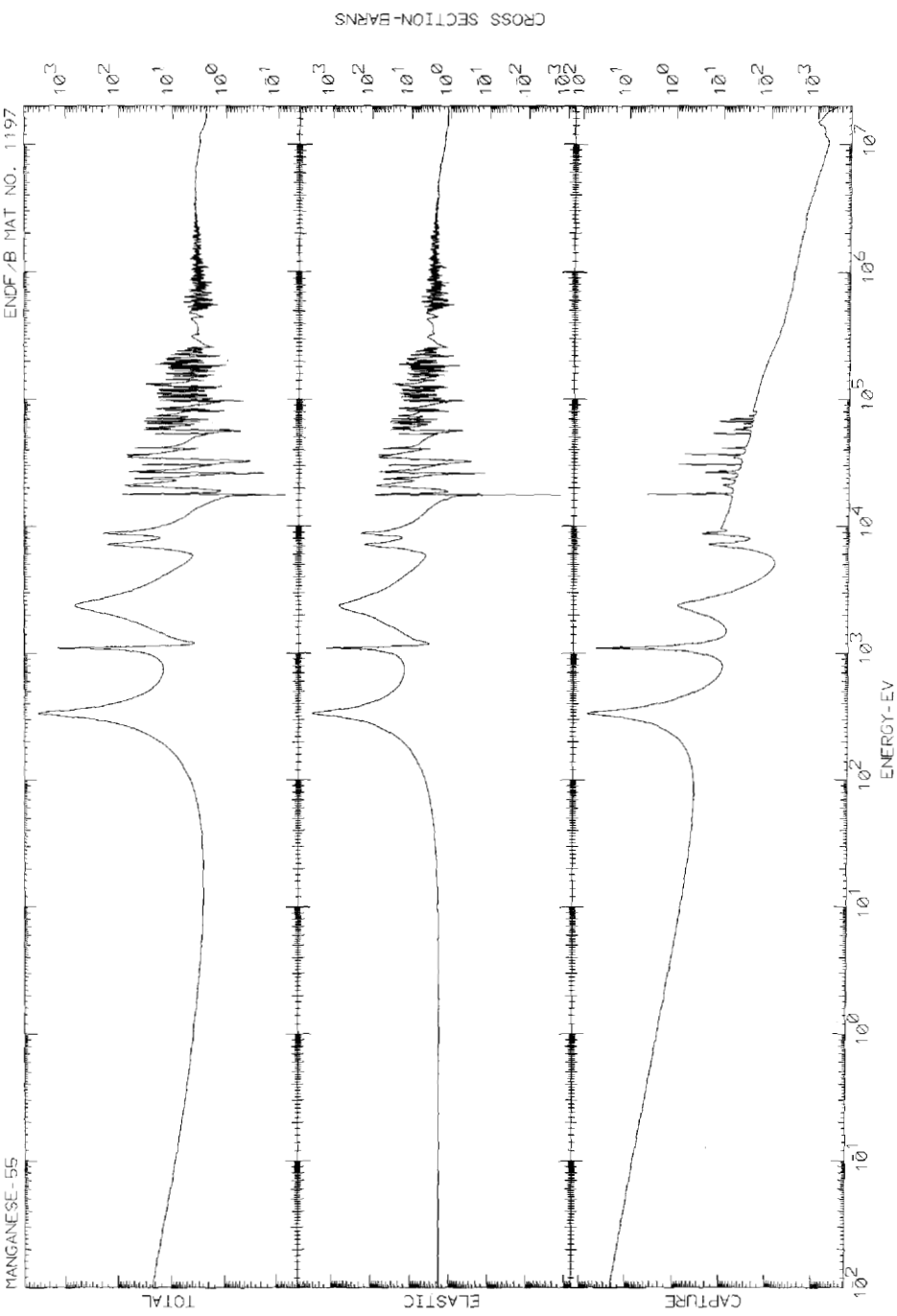

Figure 2

Total, elastic, capture cross section of ^{55}Mn.

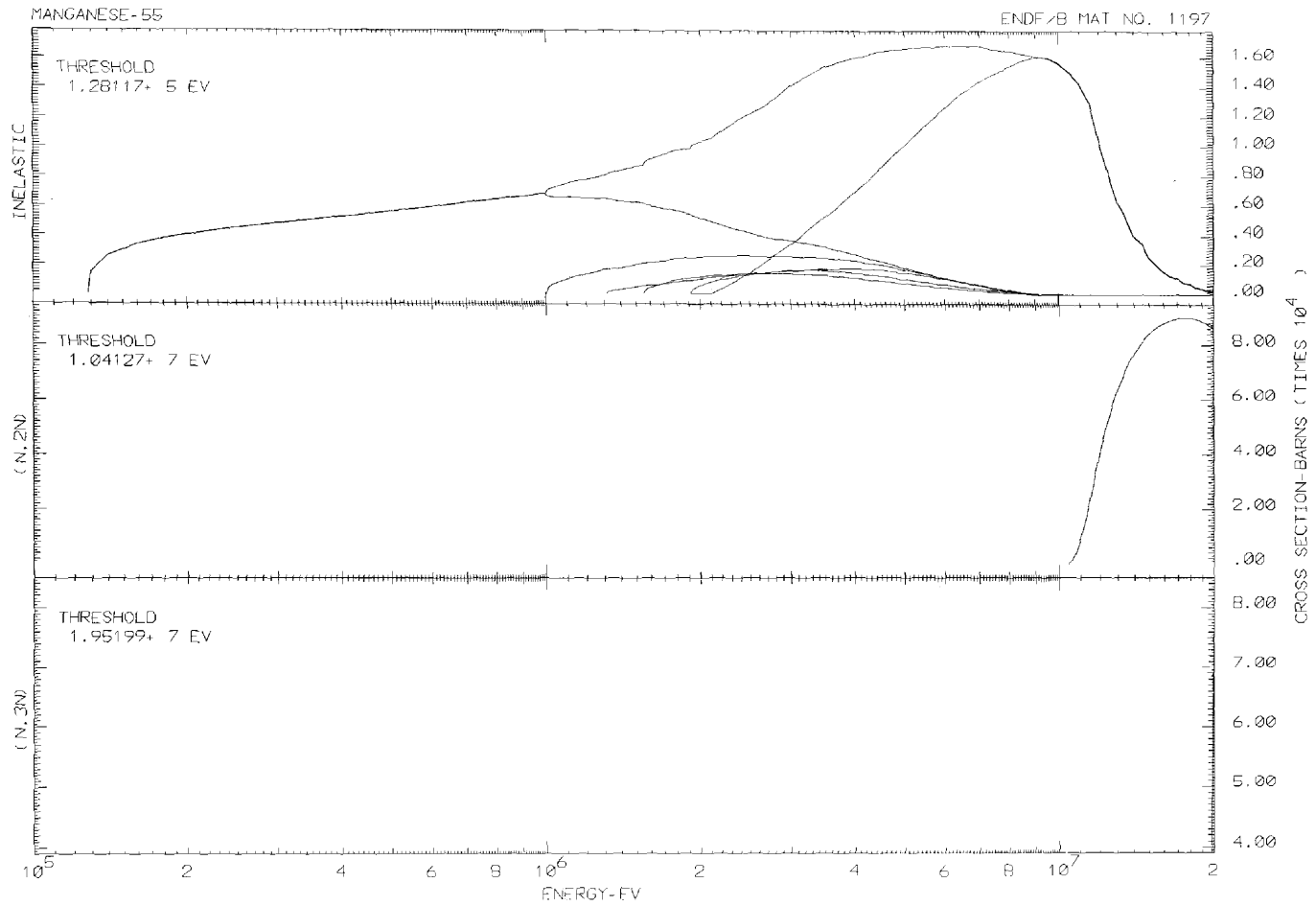

Figure 3

Total inelastic, with partial inelastic cross sections superposed, (n,2n), and (n,3n) cross sections.

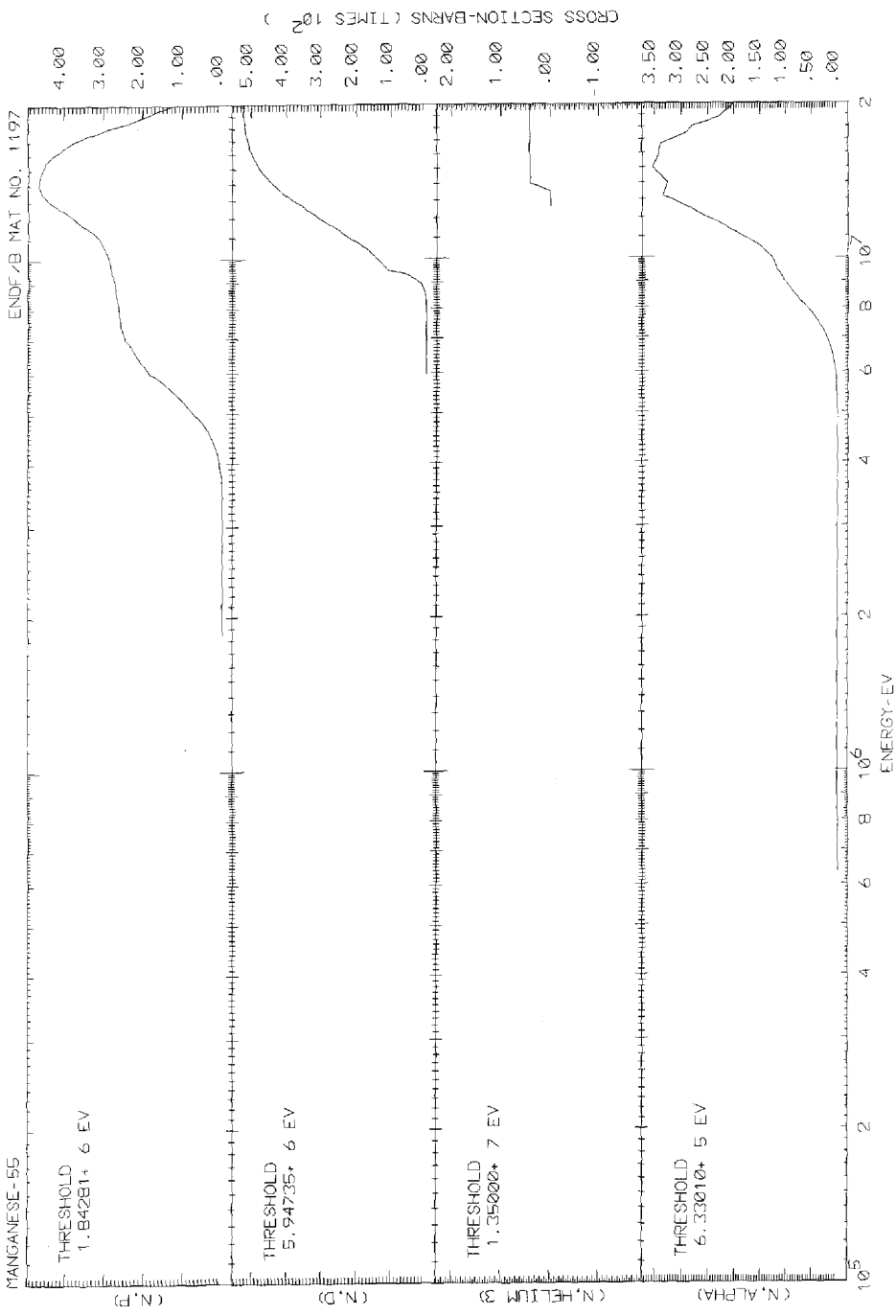

Figure 4

(n,p), (n,d), (n,^{3}He), and (n,α) cross sections.